

## Effect of Welding Heat Input on the Microstructure and Mechanical Properties of Dissimilar Friction Stir-Welded Copper/Brass Lap Joint

Farhad Gharavi<sup>a\*</sup>, Iman Ebrahimzadeh<sup>b</sup>, Kamran Amini<sup>c</sup>, Behnam Sadeghi<sup>b</sup>, Pouria Dariya<sup>b</sup>

<sup>a</sup>Department of Materials Engineering, Sirjan Branch, Islamic Azad University, Sirjan, Iran

<sup>b</sup>Advanced Materials Research Center, Department of Materials Engineering, Najafabad Branch, Islamic Azad University, Najafabad, Iran

<sup>c</sup>Department of Mechanical Engineering, Tiran Branch, Islamic Azad University, Isfahan, Iran

Received: September 02, 2018; Revised: January 10, 2019; Accepted: February 15, 2019

Dissimilar lap welded joints of copper and brass metals were fabricated by friction stir welding (FSW) method at various welding heat inputs. The effect of welding heat inputs on the microstructure and mechanical properties of overlap welded joints at two different joint configurations (i.e. Advancing side and Retreating side joint configurations) was investigated. In both joint configurations, copper and brass plates are located on the top and bottom plates, respectively. Tensile-shear and vicker's microhardness tests were conducted to evaluate the mechanical properties of dissimilar lap welded joint. In order to analysis of microstructure and fracture surface of lap welded joints, optical microscope (OM) and scanning electron microscope (SEM) were used. The obtained results showed that the weld surface of samples was appeared without groove defects, low superfluous flash and oxidation, when the welding heat input is increased. Onion ring pattern characterized by the stack of copper and brass metals is identified in the weld nugget zone (WNZ) where metal flow structures can be observed. With decreasing welding heat input, tensile-shear strength increased at both joint configurations. The highest hardness was exhibited in the WNZ with increasing welding heat input in both joint configurations.

**Keywords:** Friction Stir Welding, lap joint, Copper, Brass, Microstructure, Mechanical properties.

### 1. Introduction

Dissimilar welding of copper to brass are considered as one of the most widely used pairs of alloys in structural materials in industries such as oil and gas industries, cool and heat exchanger because of their excellent fatigue and corrosion resistance, thermal and electrical conductivity and acceptable strength<sup>1-3</sup>. The evaporation of metals with a low boiling point (such as zinc) is one of the important problem of copper to brass dissimilar welding<sup>4</sup>.

Friction stir welding (FSW) is the newest addition to friction welding (FW), a solid state welding process. Solid-state-welding-, is the change of joints- in- the- solid- states, without- fusions. Solid, state, welding, includes procedures like cold welding-, explosion welding-, ultrasonic- welding-, roll and forge welding, co- extrusion welding and FW<sup>5-7</sup>. Friction stir welding is welding' technique developed by The Welding Institute (TWI). In this technique, a non-consumable rotating welding tool is used to produce a weld where this welding tool creates frictional heat and changes the welding location and thereby affecting the change of a joint, while the material is in the solid state. The most important benefits of this technique over an arc welding techniques is that it is a solid-state process along with lower distortion, absence of difficulties regarding the melting of weld zone, higher strength of welds. FSW is successfully applied to similar

and dissimilar welding of different forms of Al alloys', steels-', titanium-, copper-' and- magnesium-, alloys as well as metal matrix composites (MMCs)-. FSW- techniques could be used in the different configuration, such as butt, corner', laps, T'-, spot-', and -fillet'' joints<sup>5-7</sup> --. Within the FSW processes, a large plastic deformation introduces to the material at an elevated temperature leading to the production of fine and equiaxed re-crystallized grains'. The resulted microstructure contributes to the excellent properties of weld in FSW process. High quality joints are considered to be due to three dimensional (3D) material flows<sup>6-7</sup>. During welding, high portion of generating heat results from the material deformation due to the tool rotation effect<sup>6-7</sup>. The peak temperature within the weld region is dependent on the used tool size, shape, rotation and traverse speed. The rotating, traverse speed and the pin size perform-a crucial role' in controlling the amount of 'heat input within the' weld region. The higher rotation speed and lower traverse speed beside heat input are expected, as well. On the contrary, the higher traverse speed and/ or lower rotating speed are considered, and then lower heat input within the weld is generated. This might not be sufficient to soften the material, resulting in an improper material flow, pin damage, and formation of defects<sup>6-7</sup>.

In previous studies, FSWdissimilar butt joints of the copper and brass alloys were investigated<sup>8-13</sup>. In this regard, Erdem<sup>14</sup> studied the microstructure and mechanical properties of copper-brass plates joined by friction stir welding. Their

\*e-mail: [fgharavi@iauirjan.ac.ir](mailto:fgharavi@iauirjan.ac.ir)

results show that the the mechanical properties and microstrain were increased by decreasing the heat input. In another paper, Barlas and uzun et al. <sup>15</sup> studied on the effect of different tool rotation speeds on microstructure and mechanical properties of friction stir butt welded dissimilar pure copper/brass alloy plates. They found that, the tool rotation speeds had effect on average grain size and onion ring formation of WNZ that by increasing the tool rotation speeds the average grain size of WNZ were decreased. Also, Moghaddam, and et al. <sup>16</sup> studied on the effect of various feed speeds on microstructure and mechanical properties of friction stir welded Cu-30Zn brass alloy. They found that, grain size profile was dependent of feed speed and the hardness values decreased by increase in feed speed.

Nowdays, researchers have studied on the FSW lap joints in dissimilar alloys. Recently, pourali and et al. <sup>17</sup> studied the influence of welding parameters on intermetallic compounds formation in lap welded dissimilar St37steel and Al 1100 alloy plates by friction stir welding. They reported that the low welding speeds and high rotational speeds where both factors were both effective factors on heat input, allowing to achieve to a good metallurgical bonding and mechanical mixing. Lee and et al. <sup>18</sup> were investigated the lap joint properties of FSWed dissimilar formed 5052 Al and 6061 Al alloys. They found that the joint strengths of FSWed lap joints mainly depended on the interface morphology and vertical transport of each material with different welding conditions. In lap joint FSW, the materials movement with weld metal due to interface of the plates and vertical transport of materials at longitudinal axis of the weld is very important. In this process, the mechanical properties, microstructure and various interfaces with different welding conditions such as transverse and rotation rate of tool, and fixing location of welded materials, were not clearly evaluated.

According to the above studies and the importance of dissimilar welding of copper to brass in the advanced cooling systems such as radiators and coolers in diesel engines instead of aluminum fittings in automotive industries, in this study, the effect of heat input on the microstructure and mechanical properties of dissimilar welding between copper and brass metals were investigated with friction stir welding process by lap joint.

## 2. Experimental Procedure

In this research, copper and brass (CuZn40) plates were used as base metals. The chemical composition of base metals is presented in Table 1. The FSW process were performed between copper and brass plates with the 300 mm×100 mm×5 mm dimensions. Welding process were conducted using a welding system equipped with a pin tool made of H13 hot work tool steel with 120 mm length, 25 mm diameter. The stirrer tip had 4.8 mm length, 9 mm diameter with M7 screw. The tool due to dipped better to welded zone were

**Table 1.** The chemical composition of base metals was used in this paper (Wt. %).

	Cu	Zn	Ni	Pb	Fe
Copper	Balance	-	-	-	-
Brass	61.27	38	0.5	0.08	0.15

made with a concave shoulder surface by an angle of  $\alpha=5^\circ$  to provide compressive force to the stirred weld zone. The length and diameter of the shoulder were 35.2 mm and 16 mm, respectively. The image and characterization of pin tool is presented in Fig. 1.

The welding process was performed using the milling machine. In this study, two different rotation rates of 710 and 450 rpm and two various feed transverse rates of 16 and 25 mm/min were used. In this study, FSW process was divided into cases A and B. Case A refer to the friction stir lap joint configuration which is copper plate is located on top plate as the advancing side (AS) and brass plate is located on the bottom plate as the retreating side (RS). Case B refer to the friction stir lap joint configuration of copper located on top plate as the retreating side and brass on the bottom plate at the advancing side as schematically shown in Figs. 2a and 2b. The welding parameters are reported in Table 2.

Two important parameters were used as variable parameters in this study, i.e. rotation ( $\omega$ ) and transverse ( $v$ ) rates. Specifications of the welding parameters are presented in Table 2. It should be noted that the speed of tool rotation and movement were measured in each process. The welding heat input (HI) is calculated using Equation 1.

$$HI = \frac{\omega^2}{v \times 10^4} \quad (1)$$

Where,  $\omega$  is the rotation rate (rpm),  $v$  is the transvers rate (mm/min), and HI is the Heating Input (J/mm).

Cross-sectional specimens cut from each joint and were prepared by sanding with #60 to #3000 silicon carbide sandpaper and polished with 0.2  $\mu\text{m}$  alumina solution ( $\text{Al}_2\text{O}_3$ ), then were attacked with etched solution (10 g  $\text{FeCl}_3$  + 40 ml  $\text{H}_2\text{O}$  + 6 ml  $\text{HCl}$  + 60 ml  $\text{C}_2\text{H}_5\text{OH}$ ) for 10-15 minutes. The optical microscope (OM), and SEM in a LEO-440i model XL30 were used to examine the microstructure and fracture surface. The mechanical properties were examined with overlap shear- tensile and microhardness tests. Due to no test standards for friction stir welded lap joints, ASTM: D3164 <sup>19</sup> providing test method for strength properties of adhesively bonded joints was chosen as the reference test standard for lap shear test. Dimensions of the samples used for lap shear testing which is almost same that Dimensions used by Xei et.al <sup>20</sup>, is shown in Figure 3. As seen in Figure, there are two spacers with the same plate thickness as indicated in gray colour for each specimen in order to obtain a balance the offset axes of the lap weld samples and to minimize the bending effects during the tensile shear testing. At room

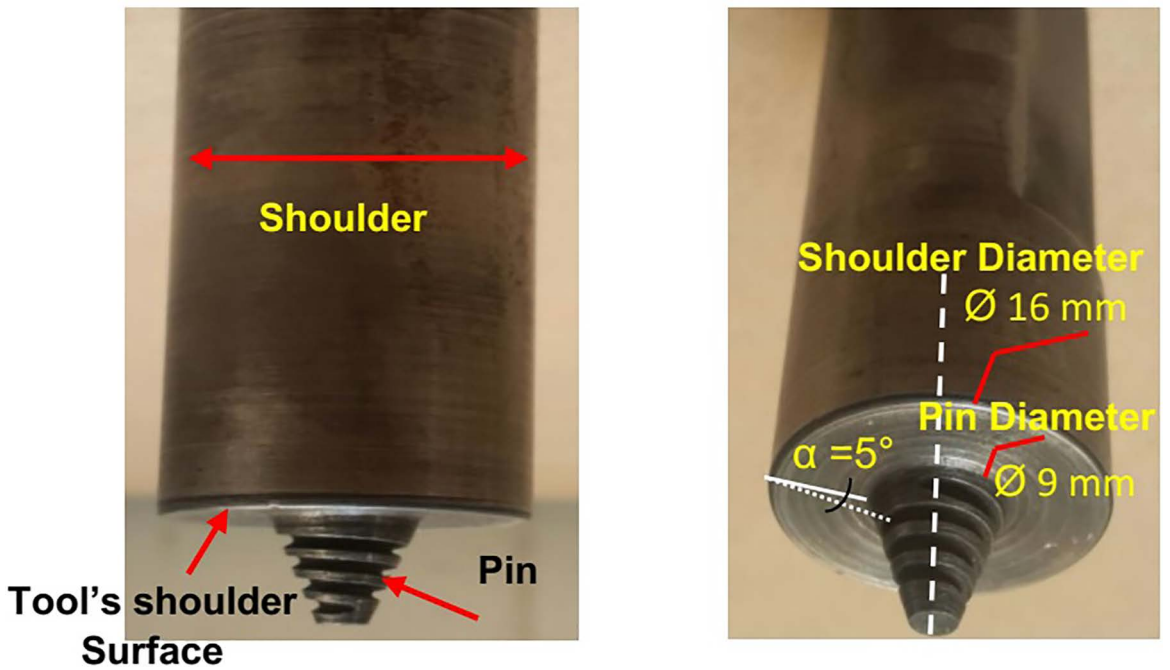


Figure 1. Geometry of the pin tool were used in this study.

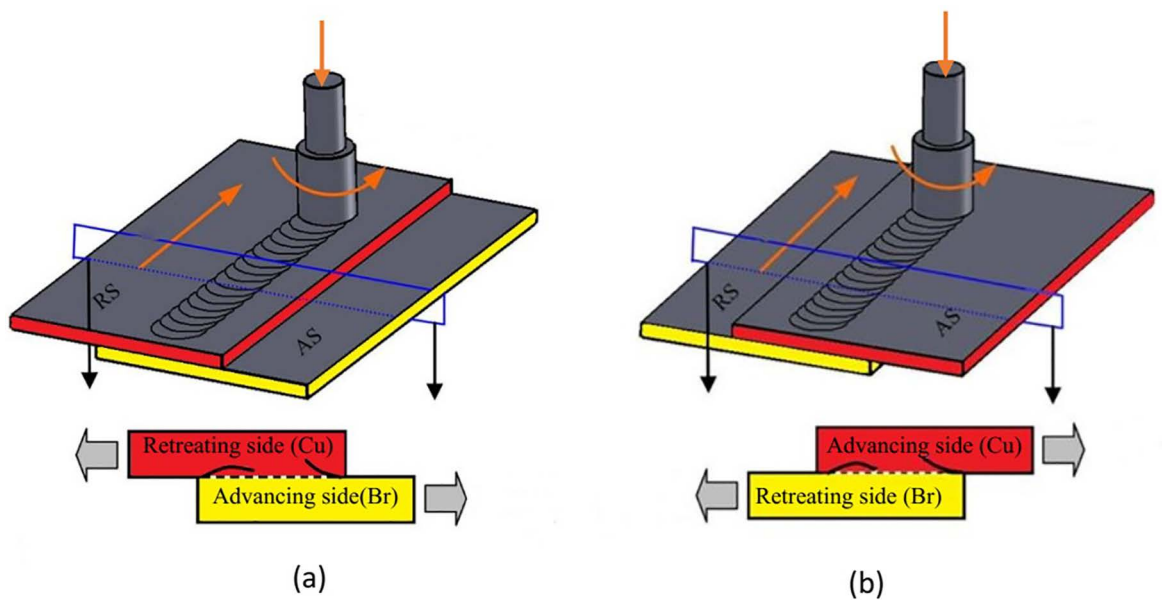
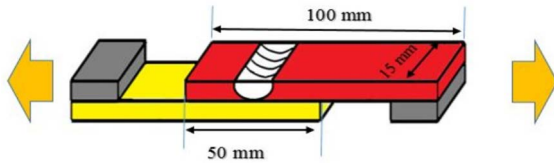


Figure 2. Schematic of FSW Cu-Brass lap joints when Cu plates were fixed on: (a) advancing side (AS), (b) retreating side (RS).

Table 2. The FSW welding parameters

Sample No.	Shoulder angle (°)	Rotation rate (rpm)	Transverse rate (mm/min)	Heat input (J/mm)
450-16	85	450	16	1.26
710-16	85	710	16	3.15
710-25	85	710	25	2.11
450-16	85	450	16	1.26
710-16	85	710	16	3.15
710-25	85	710	25	2.11



**Figure 3.** A schematic of the lap-shear tensile test specimen [20].

temperature, lap-shear tests were conducted at a strain rate of 2.0 mm/min by using a 100 KN- Instron-4486 universal testing machine. For each tensile shear testing specimen, fracture locations were recorded. Three lap shear specimens were examined to find the average weld strength for a process condition.

The horizontal Vickers micro-hardness were performed in both copper and brass side accordance with ASTM 384-05a standard. The microhardness test was performed at the load of 200 g for 10 s duration time by using Shimadzu micro indentation device.

### 3. Results and Discussion

#### 3.1 Weld Surface Feature

Surface images of lap joints between copper and brass alloys in case A with the different condition of 450 rpm- 16 mm/min, 710 rpm- 16 mm/min and 710 rpm- 25 mm/min are presented in Fig. 4. As shown in this Figure, the width of the weld region extends approximately 16 mm, equal to the shoulder diameter. All welded lap joints fabricated with the concave shoulder tool exhibit smooth surface with regularly spaced semi-circular patterns and thickness reduction relative to the original thickness of joining plates in the weld region, as a result of the contact area with the tool shoulder. The both edge of weld region are named as advancing and retreating sides. The advancing side which is denoted as AS is placed at the left side of the weld region in Figures 4. The retreating side which is denoted as RS, also, is placed at the right side of the weld region in those Figures.

Visual investigation was carried out on all welded lap joints were obtained from different welding conditions to confirm the existence of possible macroscopic external defects, such as surface irregularities, excessive flash, and lack of penetration or surface-open tunnels. The welded lap joints for all welding conditions do not display any external defects including surface irregularities and surface-open tunnels; however, some excessive flash is visible on the surface of all welded lap joints at both sides. During rotation of welding tool, the softened material moves from the RS to the AS. Accordingly, the excessive flash (or material flow arm) creates at the edge of the advancing side, as shown in Figures 4. The amount of excessive flash is dependent to the heat generated from friction between the welding tool and the material.



**Figure 4.** Surface images of lap joints between copper and brass alloys in case A with the condition of (a) 450 rpm- 16 mm/min (b) 710 rpm- 25 mm/min (c) 710 rpm- 16 mm/min

#### 3.2 Microstructural Assessment

Fig. 5 to Fig. 10 are shows the microstructure of the copper/brass FSWed joint at various welding conditions in the case A and B. Fig.5-A shows the microstructure of the copper base metal that was characterized by an  $\alpha$ -phase with deformation twins near the elongated grains, which were also observed in other works<sup>8,12</sup>. The microstructure of brass base metal was characterized by a coarse  $\alpha$ -phase in which a number of lamellar twins exist and a  $\beta$ -phase is presented in Fig. 5-E.

The grain size (Fig.5, image H) of the brass alloy in the WNZ zone is finer than that of the copper metal, while both of them represent equiaxed recrystallized grains. Copper and brass are mixed with staggered and random distribution in the WNZ zone where the grains are affected by the mechanical stirring directly. In the WNZ zone close to the brass in both sides, i.e. advancing and retreating sides (Fig. 5) a portion filled mostly by copper with little brass is found because brass at both sides brought into the WNZ zone is insufficient. However, with increasing welding heat input, there is more brass than copper and the metal flowing direction was also shown by the brass distribution at the WNZ close to the brass in both sides in all welded joints. There is no obvious change of the microstructures in the HAZ, which has also been found by other researchers<sup>8,14-21</sup>. Grain size in some portions of the HAZ at the copper side of the joint (images of B and C) decreased slightly compared with that in the BM. Welding heat input makes the deformation twins in the rolled copper plates state recrystallized, and recrystallized grains have not grown rapidly during the welding thermal cycles because of the excellent heat conductivity of copper. However, grain size in the HAZ at the brass side of the joints (images of D and G) increased slightly compared with that in the BM, because grain growth in the HAZ at the brass side is insensitive to the various welding heat input used. These actions are in contract with other obtained results from some researchers<sup>10,14,21</sup>. The grains in the TMAZ zones at both brass sides of the weld nugget zone are elongated apparently

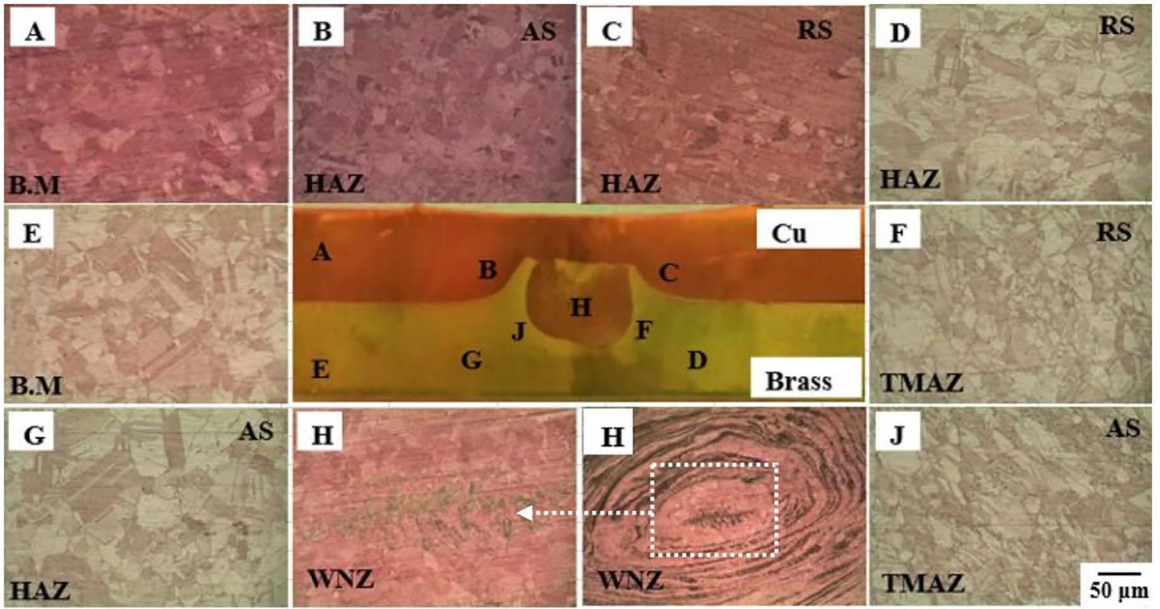


Figure 5. Optical macrostructure and microstructure of different weld zone in case A with the welding condition of 450 rpm and 16 mm/min.

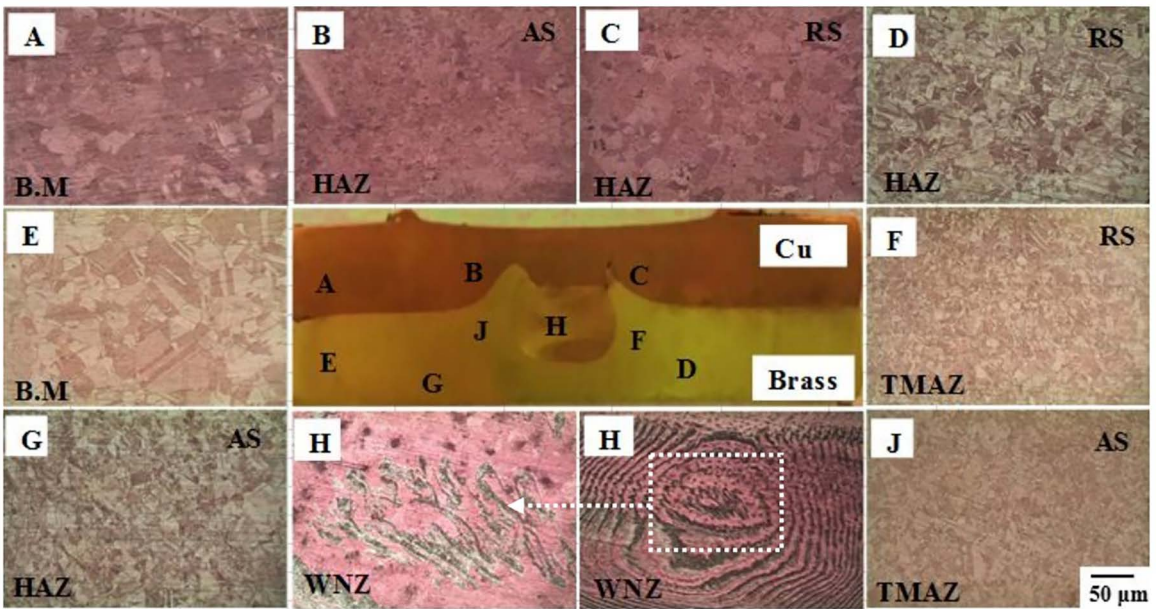


Figure 6. Optical macrostructure and microstructure of different weld zone in case A with the welding condition of 710 rpm and 25 mm/min.

by stirring force and distributed along the boundary of the WNZ zone. Some researchers documented this microstructure at TMAZ zone in the copper and brass FSWed joints<sup>16,21-23</sup>.

Image H in Figures 5 to 7 shows the onion ring patterns at various welding heat input in the AS-joint configuration. Onion ring pattern characterized by the stack of two materials is observed. Indeed, onion rings exist in the WNZ zone where metal flow structures can be observed clearly. In other words, the more complex zone exists in the middle part of the WNZ zone, so that, brass and copper grains are intertangled like onion rings. The recrystallized copper grains

in the copper band of the WNZ zone at the onion ring are greater than the brass grains in the brass band. The reason for this is the formation of excessive annealing effect of heat input on copper grains. In this regard, it is clear that with increasing welding heat input, the size of copper grains in the copper band of the WNZ zone at the onion ring are increased due to the formation of more excessive annealing effect during welding process. In all weld nugget zones, the onion ring pattern are more repeatedly observed and are mainly composed of copper metal, however, with increasing welding heat input the amount of brass alloy is increased

in the onion ring patterns. In other words, the brass band of the WNZ zone in the onion ring pattern is increased with increasing welding heat input.

Figures 8 to 10 shows the optical microstructures in the RS-joint configuration at various welding heat input. As can be seen in Fig. 8, equiaxed and fine grain structures (Image H) are also characterized in the WNZ zone of copper and brass metals. Especially, part of the onion ring stack is mainly composed of copper, which was fixed at middle of the WNZ zone. Additionally, as the welding heat input decreased, as shown in Figs.8 to 10, microstructure of the

WNZ zones represent more complex features and large part of the onion ring was brass alloy.

### 3.3 Tensile Shear properties

Table 3 and Fig. 11 show the lap shear-test results and fractured location with various welding conditions, respectively. Totally, fracture strength of AS-joint configuration was higher than the RS-joint configuration. In both AS-joint and RS-joint configuration, fracture locations were constant with various welding heat inputs and fracture always occurred at copper metal fixed on top plats at advancing side and retreating side in the AS-joint and RS-joint configurations,

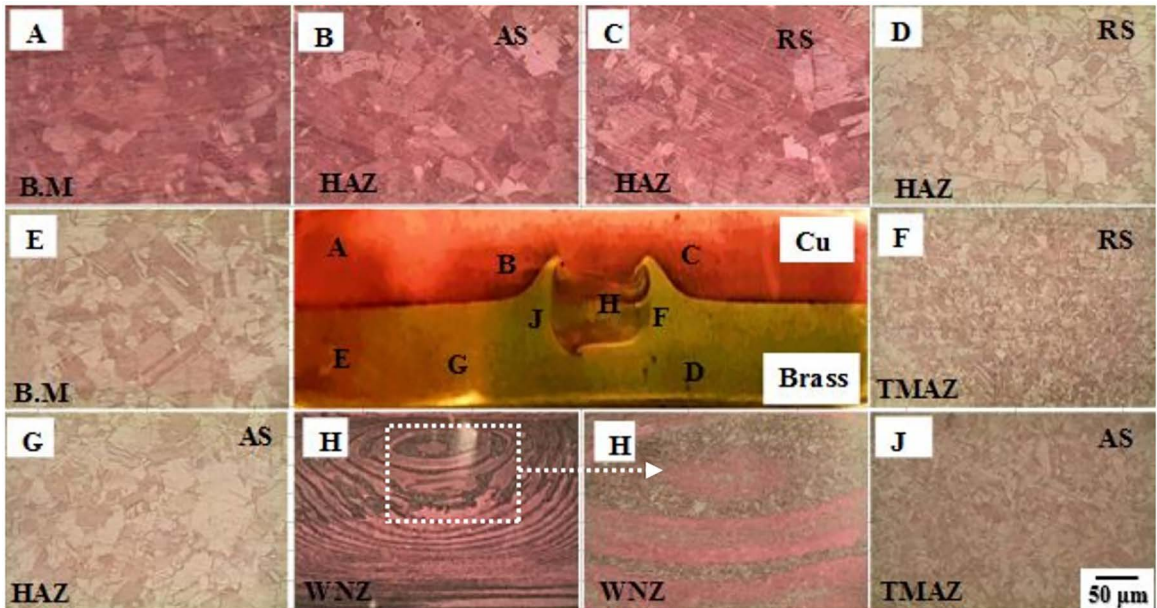


Figure 7. Optical macrostructure and microstructure of different weld zone in case A with the welding condition of 710 rpm and 16 mm/min.

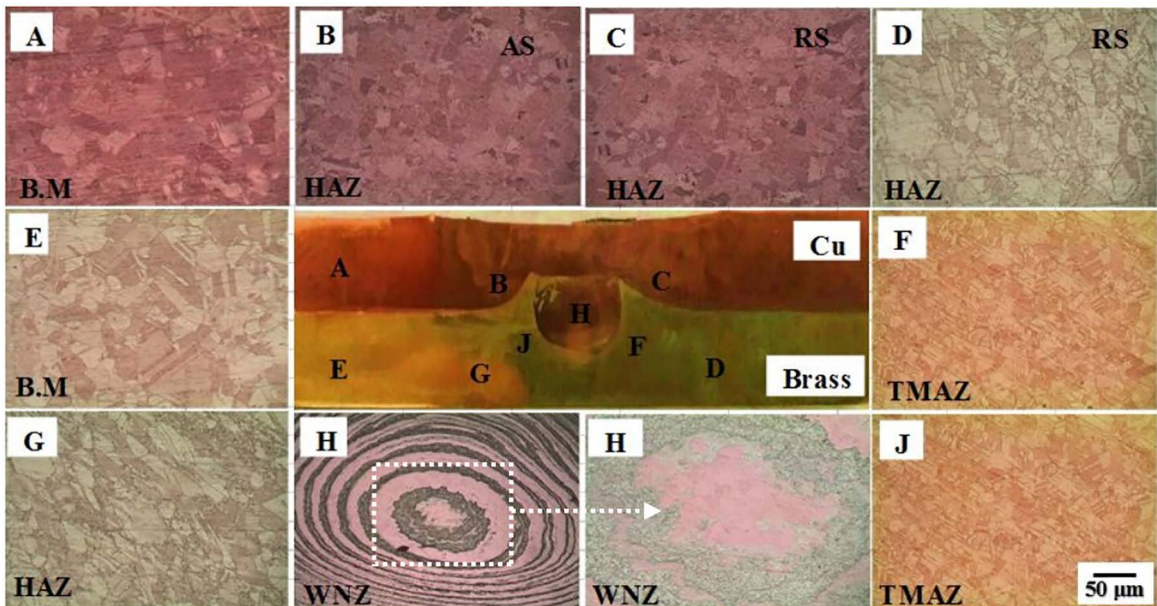


Figure 8. Optical macrostructure and microstructure of different weld zone in case B with the welding condition of 450 rpm and 16 mm/min.

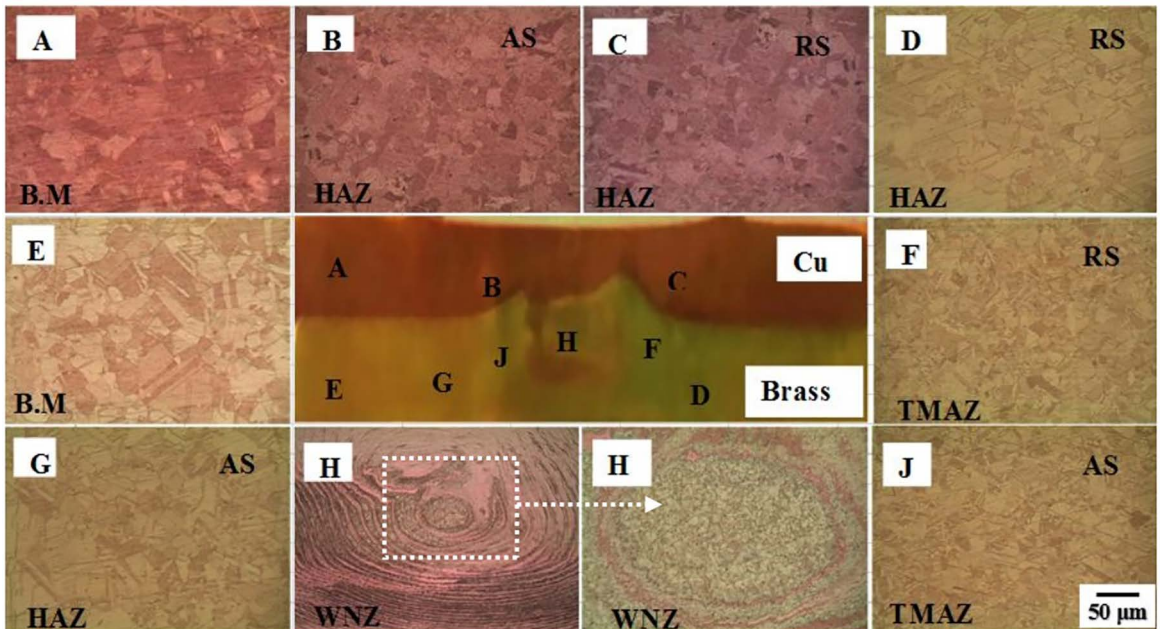


Figure 9. Optical macrostructure and microstructure of different weld zone in case B with the welding condition of 710 rpm and 25 mm/min.

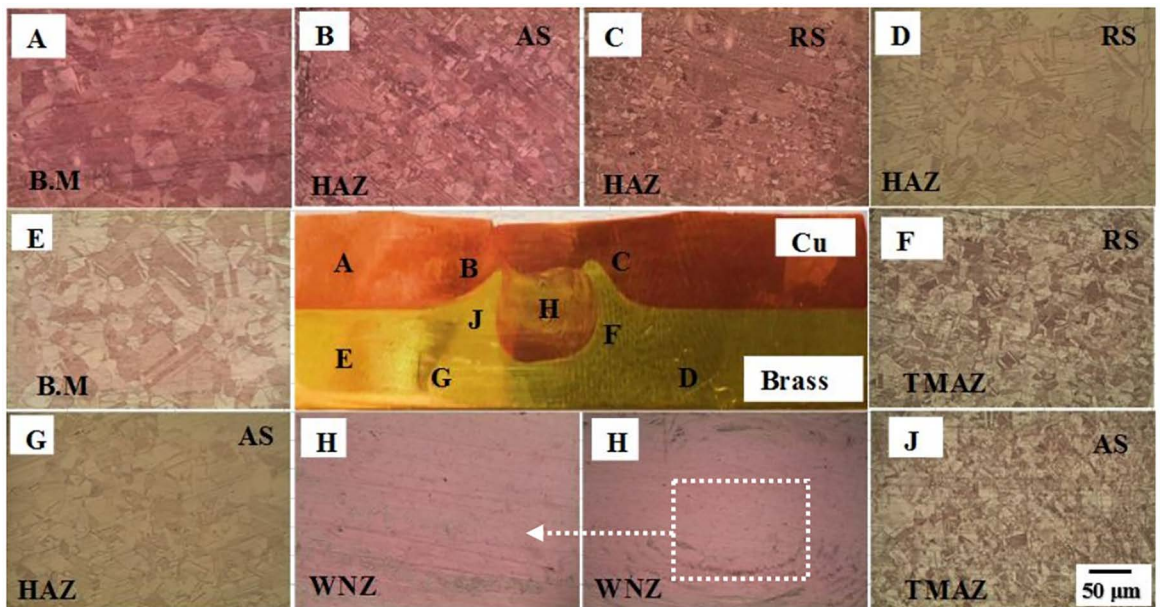


Figure 10. Optical macrostructure and microstructure of different weld zone in case B with the welding condition of 710 rpm and 16 mm/min.

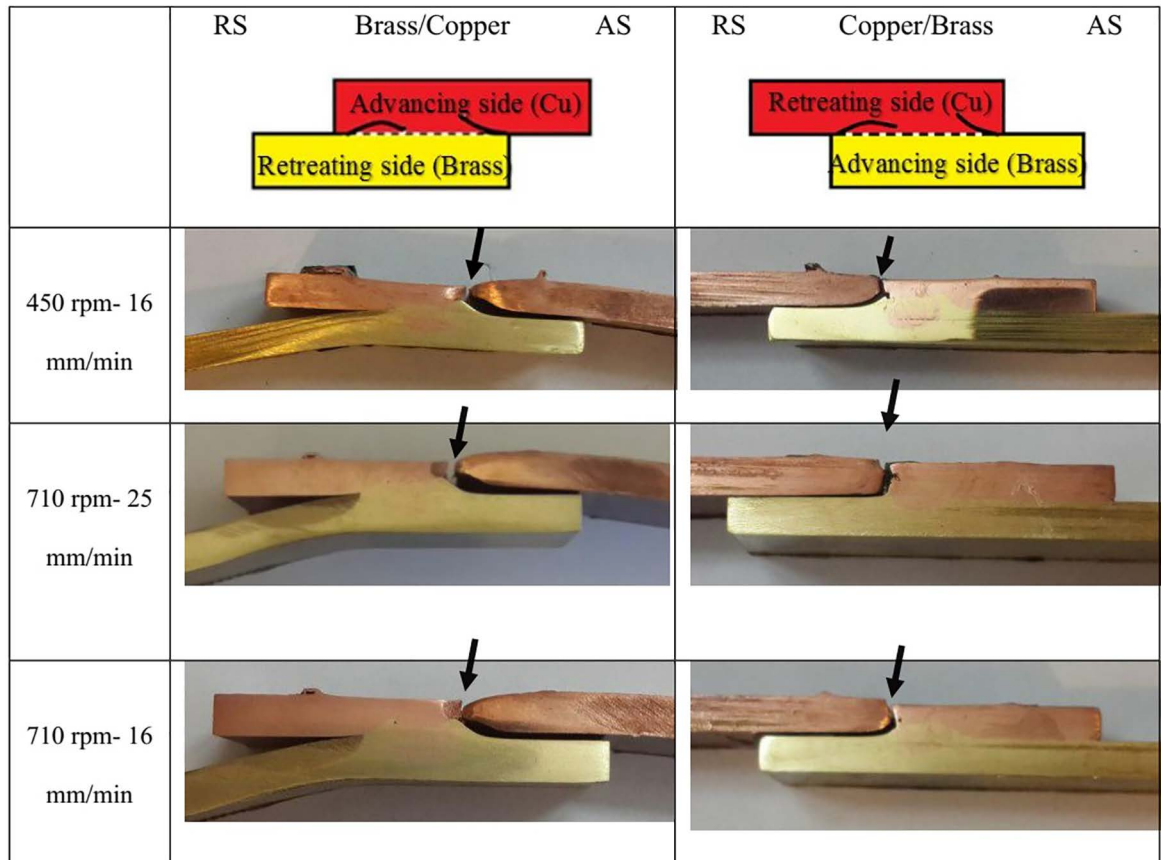
respectively. Through-nugget fracture was not observed under applied welding conditions in present research. Higher fracture strength of 174 MPa was acquired at low welding heat input (450 rpm- 16 mm/min specimen) in the AS-joint configuration.

In the RS-joint configuration, similar results depending on welding heat inputs were observed. Weak bonds were obtained under welding condition of higher welding heat input, which resulted in as much interface pull up as possible and more introduction of unbonded interface into the weld zone. As show in Fig. 11, all fractures occurred

at transition region of copper top plate, which means that the unbended region might be acted as the crack initiation site during lap shear test and responsible for lower tensile load. Because higher welding heat input resulted in fewer pull ups, the maintenance of thickness of bottom sheet of brass alloy, and less introduction of unbonded region in to the weld zone, higher fracture load was obtained and fracture occurred in a region away from the weld zone in both AS-joint and RS-joint configurations at low welding heat input. In fact, excessive vertical movement of materials can badly affect the joint strength, which means less pull-up

**Table 3.** Tensile strength of lap shear specimens

	Sample	Tensile strength (MPa)	Yield strength (MPa)	Elongation (%)
Case A	450 rpm- 16 mm/min	174	132	21
	710 rpm- 16 mm/min	153	125	18
	710 rpm- 25 mm/min	165	127	20
Case B	450 rpm- 16 mm/min	150	124	16
	710 rpm- 16 mm/min	129	111	12
	710 rpm- 25 mm/min	142	119	15

**Figure 11.** Fractured specimens after lap shear test with various welding conditions.

(less introduction of- unbonded region in to the weld zone) gives higher bond strength. In the other hand, in this research, when the deformation and heat input amounts were higher or more than the optimum values, the tensile shear strength (fracture strength) values of welded joints decreased in the both AS-Joint configurations. It can be stated that when the heat input decreased, grain size and ductility decreased and fracture strength increased.

In addition, the fracture strength values increased as the hardness of welded joints increased with decreasing welding heat input. Many studies<sup>11,20-21,24</sup> have documented the same obtained results in the welded joints of copper/brass metal with FSW process. Moreover, according to table 3, at welded joints in the both AS-joint configuration and RS-Joint

configuration have lower elongations compared to their base metals. The lower grain size of the weld regions does not agree with the lower elongation of the joints. Thus, the other phenomena may control the elongations of the joints such as higher dislocation densities of the weld regions as apposed to the base metals<sup>14,21,25</sup>. Also,  $\beta$ -phase with higher strength<sup>21,25,26</sup> in the double phase brass structure can be another reason for the lower elongation of the double phase joints. The SEM fractographs of the welded joints in the both AS-joint and RS-joint configurations are illustrated in Fig. 12 and Fig. 13, which are in complete agreement with the lower elongation of the joints.

Fig. 12 shows the SEM fractographs of fractured tensile specimens. As shown in Fig. 12 (a) to (c), the fracture surface



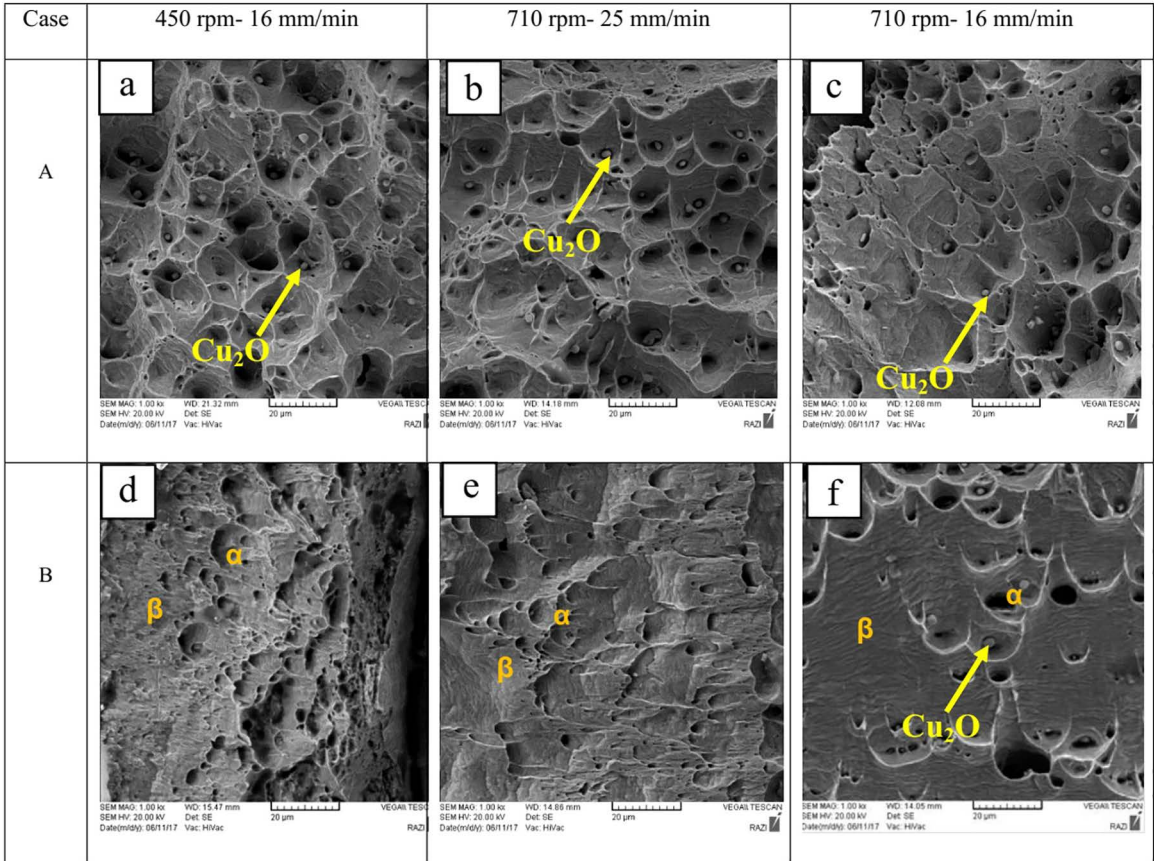


Figure 12. SEM fractographs of fractured tensile specimen.

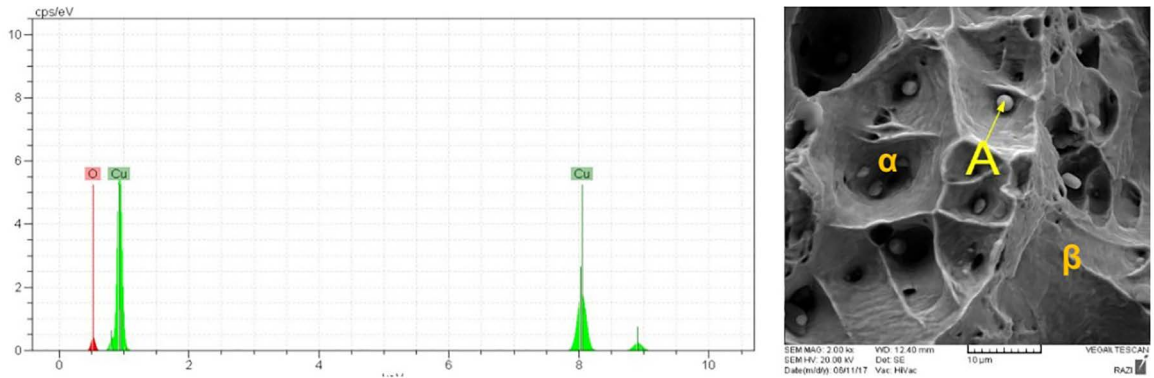


Figure 13. EDS analysis of fractured surface for 450 rpm- 16 mm/min

of the welded joints in the AS- joint configuration with various welding heat inputs contains more dimples, large voids and some feature of cleavage, therefore, the Fig. 12 shows the mixed fracture with ductile and brittle features of the weld region of welded joints. Fig. 13 shows the EDS analyzed of fractured surface for 450 rpm- 16 mm/min sample. It can be observed that amount of copper was detected on the fractured surface, especially into the dimples of welded Joint. The EDS analysis of these particles, which is showed with yellow arrow, indicates the presence of the particles on

the fractured surface. It can be concluded that the fracture occurred at the top plate near the WNZ zone. In addition, from Fig.13, the EDS analysis showed that the cleavage facets and dimples belongs to  $\beta$  and  $\alpha$  phases, respectively. Thus, it can be concluded that the lower elongation of the welded joints is due to existence of  $\beta$ - phase. On the contrary, from Fig. 12 (d) to (f), the fracture surface of welded Joints with various welding heat inputs in the RS-configuration includes fairly high dimples, large voids and more cleavage characteristics. Thus, the Fig. 12 presents the mixed fracture

with little ductile and high brittle features of welded joints. In this regard, as can be seen from Fig. 12, by increment of welding heat inputs, the cleavage facets on the fracture surface of welded joints and the size of voids and dimples are increased. Therefore, it was concluded that the fracture mechanism tends to brittle feature with increasing welding heat inputs. According to the Fig. 12 (d) to (f),  $\beta$  and  $\alpha$  phases are belonged to the cleavage facets and dimples, respectively. Furthermore, the existence of Cu particles on the fracture surface of welded joint with high welding heat input are determined with the EDS analysis (Fig. 13).

### 3.4 Microhardness profile

Fig. 14 shows the microhardness distributions near the weld zone in the midlines of the both the top and the bottom sheet with various welding conditions in two case A and case B.

Fig. 14 (a) represents the microhardness distribution in the middle of copper plate on the top plate with various welding conditions in case A. Microhardness of copper base metal shows a range of 48-50 HV, while the weld zone shows a hardening region which spreads 16mm from the weld center

regardless of the advancing and retreating sides. The central weld zone including 8-mm region from the center shows a sharply higher value, 170 HV, than that (75 HV) of a lower hardness region, which was located 16-mm away from the weld center. These results are similar to previous studied on microhardness distribution of FSWed copper/ brass metals welds zone<sup>10,14,22</sup>. As can be seen from Figure 14, it is clear that the hardness in the BM of brass is higher than that of copper, and the highest hardness can be observed in the WNZ region. This shows that the microhardness value in the WNZ zones is increased with decreasing welding heat input. However, in the copper plate, the variation of hardness value in the weld region is almost same in the middle and high welding heat inputs. In addition, the width of the indented region is almost the same in all welded joints of the weld zone, but the microhardness value of this region is increased with decreasing welding heat input. These variations are quiet evident when the welding heat input is decreased, especially in the brass or bottom plate. Indeed, in both top and bottom plates, the amount of microhardness in the HAZ at the RS-side is slightly increased rather than the microhardness in the HAZ at the AS-side in all welded

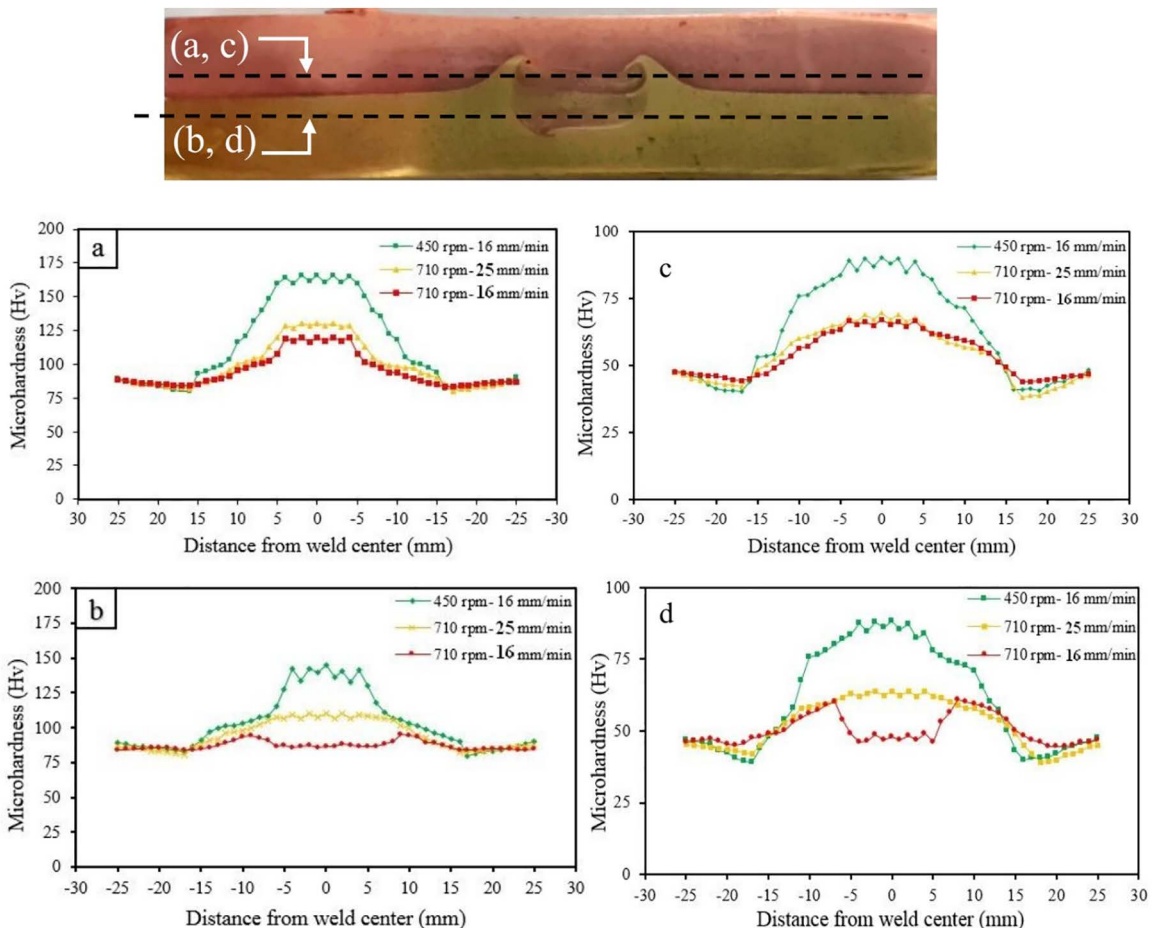


**Figure 14.** Microhardness profile near the weld zone in the midlines of the both the top and the bottom sheet with various welding conditions: (a) and (b) in case A, (c) and (d) in case B.

samples regardless of welding heat inputs. In general, the microhardness of top plate is lower than that of the bottom plate, because the wider area of weld region is located in the bottom plate, moreover, the lowest microhardness distributes in the top and bottom plates at the base metal and HAZ zone of all welded samples.

The microhardness value is closely related to the grain size. The grain refined most significantly in the WNZ zone, so the microhardness in the WNZ zone is the highest with welding heat inputs. While the microhardness was increased in the HAZ zone of brass at the bottom plate results from recrystallization - induced grain refinement, the microhardness was decreased in the HAZ zone of the copper at the top plate can be explained by the effect of annealing caused by the thermal cycle during the FSLW process. On the other hand, since, in the WNZ zone, the recrystallized copper and brass grains were present together (see Figs. 5-10, image H), slightly decreases and increases were observed in the microhardness distribution in the top and bottom plates of all welded samples. The decrease in hardness was in the zones of recrystallized copper grains, while the increase was in the zones of recrystallized brass grains. In the WNZ zone of Cu-brass plates joint with low welding heat input i.e.450 rpm/min-16 mm/min) parameter, the lowest hardness value of copper grains was 163HV, and the hardness value of brass grains was 168 HV. However, In the WNZ zones of plates were joined with high welding heat input (710 rpm-16 mm/min sample), the highest microhardness value of brass grains was 120 HV, and the microhardness value of grains was 115 HV. In general, in the bottom plate, when moving from brass (BM) towards the WNZ, microhardness value increases. However, the recrystallization in the brass grains at HAZ near the BM of brass was regional (Figs. 5-10, images of D and G). For this reason, the hardness of recrystallized brass grains, which were not recrystallized, was between 85 and 105 HV. These results showed that the hardness value of recrystallized grains in the brass transition zone was greater than the BM of brass hardness value with no recrystallized grains.

In contrast, Figs. 14 (c) and (d) represents microhardness distribution on the middle of top and bottom plates in the case of A and B with various welding condition. Similarly, Fig. 14 (c), the welded region shows a hardening zone which spreads 16-mm from the weld center regardless of both AS and RS- sides. Minimum microhardness of the weld zone is 48 HV and 85 HV in the top and bottom plates, respectively. Similar to the case A-joint configuration, higher microhardness was measured in the WNZ zone at condition of low welding heat input and in the WNZ, the recrystallized copper and brass grains were present together, more slightly decrease and increases appeared in the microhardness distribution at the top and bottom plates of all welded samples. The decrease in microhardness also was in the zones of recrystallized copper

grains with wider area, while the increase was in the zones of recrystallized brass grain with wider area, as opposed to the case A-joint configuration. Further more, from Fig. 14 (c) and (d), it is important to note that with increasing welding heat inputs, the microhardness value in the weld region is sharply decreased, especially in the WNZ zone. This is related to the existence of coarse grains with lower angle grain boundary and lower density of dislocation in the WNZ zone at the both top and bottom plates. As matter of fact, the microhardness value directly depends on the grain size. Thus, with increasing welding heat input, especially at high heat input, the grain size is sharply increased in the weld region and in the WNZ zone, due to the higher temperature than the other regions, the grain size is reduced and the hardness value is extremely decreased. Indeed, another reason to decreased hardness value in the WNZ at of high welding heat input is related to decrease of recrystallized brass grains and to increase of not crystallized and coarsening copper grains due to the annealing effect which is caused by more thermal cycle during FSW process with high heat input. (see Fig. 14).

#### 4. Conclusions

In this study, the effect of welding heat input on microstructure, mechanical properties of dissimilar lap welded of copper to brass were evaluated, and the following results were obtained:

1. Surface feature of the welded joints was observed without groove defects, low superfluous flash and oxidation with increasing welding heat input.
2. Microstructural evaluations were depicted: the weld cross section contained four different zones (BM, HAZ, TMAZ, and WNZ). In the WNZ, copper and brass metals are mixed together and they cause the more complex zone in the middle part of the WNZ, so that brass and copper grains are inter tangled like onion ring. At both joint configurations, with decreasing welding heat input, the WNZ clearly observed with more complex features and large part of the onion ring was brass alloy.
3. At both AS- joint and RS-joint configurations, the grain size and elongation decreased and tensile-shear-strength increased when the heat input decreased.
4. SEM fractographs of fractured tensile samples showed that the mixed fracture with little ductile and high brittle features is formed and at both joint configurations, by increase of welding heat input, the cleavage faces on the fracture surface of welded joints, the size of voids, and dimples are enhanced in both configurations.
5. The higher microhardness was measured in the WNZ at condition of low welding heat input in the both joint configurations.

## 5. References

1. Johnsen MR. Friction Stir Welding Takes off at Boeing. *Welding Journal*. 1999;78(2):35-39.
2. Mendez PF, Eager TW. *Welding Processes for Aeronautics. Advanced Materials and Processes*. 2001;159:39-43.
3. Burford D, Widener C, Tweedy B. Advances in Friction Stir Welding for Aerospace Applications. In: 6th AIAA Aviation Technology, Integration and Operations Conference (ATIO); 2006 Sep 25-27; Wichita, KS, USA.
4. Akbari Mousavi SAA, Niknejad ST. An Investigation on Microstructure and Mechanical Properties of Nd:YAG Laser Beam Weld of Copper Beryllium Alloy. *Metallurgical and Materials Transactions A*. 2009;40(6):1469-1478.
5. Mishra RS, Ma ZY. Friction stir welding and processing. *Materials Science and Engineering: R: Reports*. 2005;50(1-2):1-78.
6. Nandan R, DebRoy T, Bhadeshia HKDH. Recent advances in friction-stir welding - Process, weldment structure and properties. *Progress in Materials Science*. 2008;53(6):980-1023.
7. Padhy GK, Wu CS, Gao S. Friction stir based welding and processing technologies - processes, parameters, microstructures and applications: A review. *Journal of Materials Science & Technology*. 2018;34:1-38.
8. Park HS, Kimura T, Murakami T, Nagano Y, Nakata K, Ushio M. Microstructures and mechanical properties of friction stir welds of 60% Cu-40% Zn copper alloy. *Materials Science and Engineering: A*. 2004;371(1-2):160-169.
9. Sun YF, Fujii H. Investigation of the welding parameter dependent microstructure and mechanical properties of friction stir welded pure copper. *Materials Science and Engineering: A*. 2010;527(26):6879-6886.
10. Meran C. The joint properties of brass plates by friction stir welding. *Materials & Design*. 2006;27(9):719-726.
11. Lee WB, Jung SB. The joint properties of copper by friction stir welding. *Materials Letters*. 2004;58(6):1041-1046.
12. Zhang YN, Cao X, Larose S, Wanjara P. Review of tools for friction stir welding and Processing. *Canadian Journal of Metallurgy and Materials Science*. 2012;51(3):250-261.
13. Thomas WM, Lockyers SA, Kalee SW, Staines DG. Friction stir welding - an update on recent developments. In: *Proceedings of Conference on Stressed Components in Aluminum Alloys*; 2003 Apr 2; Birmingham, UK.
14. Erdem M. Investigation of structure and mechanical properties of copper-brass plates joined by friction stir welding. *International Journal of Advanced Manufacturing Technology*. 2015;76:1583-1592.
15. Barlas Z, Uzun H. Microstructure and mechanical properties of friction stir butt-welded dissimilar pure copper/brass alloy plates. *International Journal of Materials Research*. 2010;101(6):801-807. DOI: 10.3139/146.110340
16. Moghaddam MS, Parvizi R, Haddad-Sabzevar M, Davoodi A. Microstructural and mechanical properties of friction stir welded Cu-30Zn brass alloy at various feed speeds: influence of stir bands. *Materials & Design*. 2011;32(5):2749-2755.
17. Pourali M, Abdollah-Zadeh A, Saeid T, Kargar F. Influence of welding parameters on intermetallic compounds formation in dissimilar steel/aluminum friction stir welds. *Journal of Alloys and Compounds*. 2017;715:1-8.
18. Lee CY, Lee WB, Kim JW, Choi DH, Yeon HM, Jung SB. Lap joint properties of FSWed dissimilar formed 5052 Al and 6061 Al alloys with different thickness. *Journal of Materials Science*. 2008;43(9):3296-3304.
19. ASTM International. ASTM D3164-03 - Standard Test Method for Strength Properties of Adhesively Bonded Plastic Lap Shear Sandwich Joints in Shear by Tension Loading. West Conshohocken: ASTM International; 2003.
20. Xie GM, Ma ZY, Geng L. Development of a fine-grained microstructure and the properties of a nugget zone in friction stir welded pure copper. *Scripta Materialia*. 2007;57(2):73-76.
21. Zhou L, Zhou WL, Feng JC, He WX, Huang YX, Dong SS. Effect of rotation speed on the microstructure and mechanical properties of dissimilar friction stir-welded copper/brass metals. *International Journal of Advanced Manufacturing Technology*. 2016;84(5-8):1335-1343. DOI: 10.1007/s00170-015-7792-9
22. Zhang Z, Zhang HW. A fully coupled thermo-mechanical model of friction stir welding. *International Journal of Advanced Manufacturing Technology*. 2008;37(3-4):279-293.
23. Ramesh S. Physical Effect of Heat on Material During Welding. In: *Ramesh S. Applied Welding Engineering - Processes, Codes, and Standards*. Waltham: Butterworth-Heinemann; 2012. p. 171-174.
24. Barekatin H, Kazeminezhad M, Kokabi AH. Microstructure and Mechanical Properties in Dissimilar Butt Friction Stir Welding of Severely Plastic Deformed Aluminum AA 1050 and Commercially Pure Copper Sheets. *Journal of Materials Science & Technology*. 2014;30(8):826-834.
25. Heidarzadeh A, Saeid T. A comparative study of microstructure and mechanical properties between friction stir welded single and double phase brass alloys. *Materials Science and Engineering: A*. 2016;649:349-358.
26. Emami S, Saeid T. Effects of Welding and rotational speeds on the Microstructure and Hardness of Friction Stir Welded Single-Phase Brass. *Acta Metallurgica Sinica (English Letters)*. 2015;28(6):766-771.